International Journal of Biological Macromolecules 156 (2020) 783–791

Contents lists available at ScienceDirect

International Journal of Biological Macromolecules

journal homepage: http://www.elsevier.com/locate/ijbiomac

Formulation, characterization and *in vitro* release study of 5-fluorouracil loaded chitosan nanoparticles

Moshera Samy [a,*], Sameh Hosam Abd El-Alim [b], Abd El Gawad Rabia [c], Amal Amin [a], Magdy M.H. Ayoub [a]

[a] Polymers and Pigments Department, National Research Centre, Dokki 12622, Giza, Egypt
[b] Pharmaceutical Technology Department, National Research Centre, Dokki 12622, Giza, Egypt
[c] Chemistry Department, Faculty of Science, Ain Shams University, Cairo, Egypt

ARTICLE INFO

Article history:
Received 13 March 2020
Received in revised form 9 April 2020
Accepted 14 April 2020
Available online 19 April 2020

Keywords:
Ionic gelation
Chitosan
5-Fluorouracil

ABSTRACT

The main objective of this study was to evaluate the most suitable conditions to prepare 5-fluorouracil (5-FU) loaded chitosan nanoparticles (CSNPs). 5-FU loaded CSNPs were prepared employing the ionic gelation technique using three different molecular weights of CS with the polyanion sodium tripolyphosphate (STPP) as cross-linking agent. The preparation was based on the ionic interaction of positively charged CS and negatively charged STPP. The entrapment efficiency (EE%) of CSNPs was in the range of 3.86–21.82% EE% exhibited a clear increase with increasing CS concentration. The averge particles size was in the nanosize range and monodisperse in nature whereas transmission electron microscope micrographs showed that the prepared nanoparticles have a spherical shape. Fourier transform infrared (FTIR), X- ray differaction (XRD) and differential scanning calorimetry (DSC) confirmed successful incorporation of 5-FU in prepared CSNPs. *In vitro* release of 5-FU from selected formulations exhibited sustained release from the nanoparticles where slower release was observed when higher molecular weight CS was used. The study of drug release kinetics revealed that the release of 5-FU from CSNPs followed a diffusion controlled pattern.

1. Introduction

5-fluorouracil (5-fluoro-2,4-pyrimidinedione, 5-FU) is a pyrimidine analogue which acts as an antimetabolite. It is characterized by having a broad range of activity, either alone or along with other antitumor drugs, against solid tumors of the gastrointestinal tract, ovary, pancreas, liver, head, neck, brain and breast [1–3]. Owing to its structure, 5-FU can be incorporated into RNA and DNA. It can also hamper nucleoside metabolism which ultimately leads to cytotoxicity and cell death [4]. The major disadvantages of using 5-FU include non-specificity that leads to systemic toxicity as well as its very low bioavailability and short plasma half life. This leads to the use of high doses, thus resulting in side effects [5]. In addition, development of resistance by tumor cells had greatly limited the clinical applications of 5-FU [6,7]. One of the solutions to beat these shortcoming is drug incorporation into polymeric nanoparticles. These drug delivery carriers have unique characteristics such as the ease of modification of their surface properties and the ability to protect the encapsulated drug and increase its stability [8]. Polymeric nanoparticles can also increase drug bioavailability, provide a controlled drug release pattern and increase tissue and cell selectivity [9].

In recent years, there have been a great increase in the interest of investigating nanotechnology in the field of drug delivery. Nanoparticlulate drug delivery carriers can be formulated using several types of polymers. They have the ability to incorporate different categories of chemotherapeutic agents, thus protecting them from nonspecific uptake to major organs, protein adsorption and renal clearance. A variety of biodegradable polymers have been investigated for their potential as drug delivery nanocarriers [10]. Polymeric nanoparticles are solid carriers characterized by having sizes <1 μm. They have the ability to entrap, attach or dissolve chemotherapeutic entities into their matrices [11,12]. Moreover, several reports have indicated that these nanocarriers can adjust drug release profile by altering the molecular weight and degradation rate of the polymers used in their formulation [13,14].

Chitosan (CS) is the only alkaline polysaccharide in nature. It is the product of deacetylation of chitin and is widely used in pharmaceuticals, textiles, environmental monitoring and tissue repairs [15]. CS is generally regarded as biocompatible, biodegradable and nontoxic [16]. Due to its physicochemical and biological beneficial properties, CS has been widely investigated for the development and preparation of nanoparticles [17–19]. A number of methods can be used for preparation of chitosan nanoparticles (CSNPs). These methods comprise chemical cross-

* Corresponding author at: Polymers and Pigments Department, National Research Centre, El-Buhouth Street, Dokki 12622, Giza, Egypt.
E-mail address: moshera_samy1984@yahoo.com (M. Samy).

https://doi.org/10.1016/j.ijbiomac.2020.04.112
0141-8130/

linking [20], emulsification solvent diffusion [21] and ionic gelation [22–24]. Among the variety of techniques investigated to prepare CSNPs, ionic gelation has attracted great interest as this process has the advenatges of beign controllable, convenient, free of organic solvents and non-toxic [25]. This method is based on physical cross-linking, thus it avoids possible toxicity of chemical cross-linkers or emulsifying agents. Ionic gelation also prevents the risk of damage to incorporated therapeutic agents, particularly if they are biological in nature [26]. In this approach, CSNPs are formed by means of electrostatic interactions between positively charged CS chains and polyanions, used as cross-linkers, like tripolyphosphates [27,28]. Sodium tripolyphosphate (STPP) is the most extensively used ion cross-linking agent due to its non-toxic and multivalent properties [29].

Thus, the current work aims to study various factors affecting both the formation of 5-FU loaded CSNPs and their efficiency as 5-FU carriers. The influence of parameters such as CS molecular weight, CS concentration and STPP concentration on the colloidal properties of nanoparticles prepared by ioinc gelation was investigated. Nanoparticles were tested for drug encapsulation efficiency (EE%), particles size (PS) as well as particle morphology. Moreover, incorporation of 5-FU into the prepared nanoparticles was evaluated employing Fourier transform infrared spectroscopy (FTIR), X-ray diffraction (XRD), energy dispersive X-ray spectroscopy (EDAX) and differential scanning calorimetry (DSC). The *in vitro* release pattern of 5-FU from prepared nanoparticles as well as analysis of release kinetics were performed.

2. Experimental

2.1. Materials

Three different molecular weights of chitosan (CS; $(C_6H_{11}NO_4)n$; (1,4)-2-Amino-2-desoxy-beta-D-glucan) i.e. high, medium and low (molecular weight 600,000, 300,000 and 150,000 g/mol, respectively) were obtained from Alfa Aesar, USA. 5-fluorouracil (5-FU; $C_4H_3FN_2O_2$; 5-fluoropyrimidine-2,4-dione, ≥99%) and sodium tripolyphosphate (STPP, $Na_5P_3O_{10}$), and disodium hydrogen orthophosphate (Na_2HPO_4) were obtained from Sigma-Aldrich, Germany. All other chemicals otherwise mentioned were of analytical grade.

2.2. Methods

2.2.1. Preparation of 5- fluorouracil loaded chitosan nanoparticles

5-FU loaded CSNPs were prepared employing the ionic gelation technique as previously reported by Calvo et al. [30] using CS of three different molecular weights (low, medium and high). CS solution with three different concentrations (3, 4 and 5 mg/ml, respectively) was prepared using 0.5% acetic acid. 10 mg of 5-FU was dissolved in 5 ml of CS solution followed by dropwise addition of 2.5 ml of STPP aqueous solution with different concentrations (1, 2 and 3 mg/ml) under continous stirring [31]. Accordingly, a total of 27 formulations were investigated and their composition is presented in Table 1. The obtained nanoparticle dispersion was gently stirred for 45 min at 600 rpm at room temperature to allow excess drug to adsorb to the nanoparticles and attain isothermal equilibrium [32]. Finally, the nanoparticle dispersion was centrifuged at 6.000 rpm for 60 min (K-2015 ambient centrifuge Centurion scientific, UK) and washed twice with 0.5% acetic acid. The combined washings were used to determine the drug EE% whereas the precipitated nanoparticle pellets were used for further analyses.

2.2.2. Characterization of 5-fluorouracil loaded chitosan nanoparticles

2.2.2.1. Determination of encapsulation efficiency. In order to detrmine the EE% of 5-FU in the prepared nanoparticles, the combined washings after centrifugation were appropriately diluted using 0.5% acetic acid. The amount of free, unencapsulated 5-FU was measured spectrophotometrically at 265.2 nm using the regression equation of the standard calibration curve plotted employing suitable concentrations of 5-FU [33]. The amount of encapsulated 5-FU was determined by difference between the amount of free, unencapsulated 5-FU in the combined washings and the initial amount used in preparation of CSNPs where the following equation was employed [34,35]:

$$EE\% = \frac{\text{Free drug} - \text{Total drug}}{\text{Total drug}} \times 100$$

Table 1
Formulation codes and composition of investigated 5-FU loaded CSNPs.

Formulation	CS Mw	CS (mg/ml)	STPP (mg/ml)	CS: STPP mass ratios	Visual identification
L31		3		6:1	Clear Solution
L41		4	1	8:1	Clear Solution
L51		5		10:1	Clear Solution
L32		3		3:1	Colloidal dispersion
L42	Low	4	2	4:1	Colloidal dispersion
L52		5		5:1	Colloidal dispersion
L33		3		2:1	Colloidal dispersion
L43		4	3	2.66:1	Aggregation
L53		5		3.33:1	Aggregation
M31		3		6:1	Clear Solution
M41		4	1	8:1	Clear Solution
M51		5		10:1	Clear Solution
M32		3		3:1	Colloidal dispersion
M42	Medium	4	2	4:1	Colloidal dispersion
M52		5		5:1	Colloidal dispersion
M33		3		2:1	Colloidal dispersion
M43		4	3	2.66:1	Aggregation
M53		5		3.33:1	Aggregation
H31		3		6:1	Clear Solution
H41		4	1	8:1	Clear Solution
H51		5		10:1	Clear Solution
H32		3		3:1	Colloidal dispersion
H42	High	4	2	4:1	Colloidal dispersion
H52		5		5:1	Colloidal dispersion
H33		3		2:1	Aggregation
H43		4	3	2.66:1	Aggregation
H53		5		3.33:1	Aggregation

2.2.2.2. Determination of particle size. The PS for the prepared nanoparticles was measured by means of photon correlation spectroscopy using a zeta-sizer (Nano ZS, Malvern Instruments Ltd., Malvern, UK). Samples were suitably diluted with distilled water and measured at ambient temperature using quartz cuvettes.

2.2.2.3. Fourier transform infrared spectroscopy. FTIR spectroscopy was used to study the spectra of 5-FU, CS, STPP as well as the selected 5-FU loaded CSNPs. The spectra were recorded using FTIR spectrometer (Jasco, FT/IR 6100, Japan). The KBr pellet method was employed where the powdered samples were ground and mixed with KBr then compressed into discs. A scanning range of 4000–400 cm^{-1} was employed.

2.2.2.4. X-ray diffraction. The physical state of 5-FU, CS, STPP and selected 5-FU loaded CSNP formulations was evaluated using X-ray diffraction. Measurements were acquired with X-ray diffractometer (Bruker AXS, D8 Advance, Germany) which was operated at 40 KV and 40 mA using CuKα as a radiation source where λ = 1.54 A°. The diffractograms were recorded in the diffraction angle (2θ) range between 4 and 50° and the process parameters were set at scan step size of 0.020° and scan step time of 0.4 s.

2.2.2.5. Differential scanning calorimetry. Thermal analysis of 5-FU, CS (low, medium and high molecular weight), STPP and selected 5-FU loaded CSNPs formulations was performed by Perkin-Elmer differential scanning calorimeter (Shimadzu, DSC-60, Japan). The samples were scanned at a temperature that ranged from 20 °C to 400 °C, with a

Table 2
EE%, PS and PDI values of investigated 5-FU loaded CSNPs.

Formulation	EE% ± SD	PS (nm) ± SD	PDI
L32	7.45 ± 1.73	319.1 ± 40.62	0.127
L42	8.33 ± 1.76	377.7 ± 47.29	0.125
L52	21.82 ± 3.64	484.3 ± 82.49	0.380
M32	3.86 ± 0.33	379.9 ± 74.44	0.196
M42	6.95 ± 0.77	324.6 ± 45.36	0.269
M52	16.66 ± 1.34	631.7 ± 270.2	0.234
H32	7.35 ± 1.34	426.5 ± 54.29	0.127
H42	6.15 ± 2.61	512.5 ± 109.6	0.302
H52	21.12 ± 1.25	529.2 ± 85.85	0.346

scan rate of 10 °C/min and the analysis took place in aluminum pans, under nitrogen atmosphere using reference alumina.

2.2.2.6. Energy dispersive X-ray spectroscopy analysis. Energy dispersive X-ray spectroscopy (EDAX) was used for identifying the elemental composition of selected 5-FU loaded CSNP formulations. The freeze dried samples were analyzed by energy dispersive X-ray spectroscopy (Quanta FEG 250-FEI, Holland). The atomic and weight percentage of the existing elements was calculated by using EDAX spectrum.

2.2.2.7. Transmission electron microscopy. The morphology of a selected 5-FU loaded CSNP formulation and its dimensions in nanometer range was confirmed by TEM. The transmission electron microscope (JEOL Co., JEM-2100, Japan) was adjusted at a high tension electricity of 200 kV. One drop of the appropraitely diluted sample was placed onto a carbon-coated copper grid, negatively stained with 1% phosphotungstic acid and left to dry at ambient temperature before being examined at suitable magnifications.

2.2.3. In vitro drug release study

The *in vitro* release of 5-FU, in free form and from selected prepared CSNPs, was evaluated employing the dialysis bag technique [32] using a dialysis tubing cellulose membrane (Visking®, SERVA Electrophoresis GmbH, Germany; Molecular weight cutoff 12.000–14.000). An amount equivalent to 2 mg of 5-FU was instilled in the dialysis bag, sealed at both ends to prevent leakage and placed in screw-capped glass containers filled with 50 ml phosphate buffer (pH 7.4). The entire system was kept at 37 ± 0.5 °C at 100 rpm using a shaking water bath. At predetermined time intervals (1, 2, 3, 4, 6, 8, 24 and 48 h), 5 ml of the release medium was withdrawn and replaced with 5 ml of fresh buffer solution. The samples were adequately diluted and analyzed for 5-FU content spectrophotometrically at 266.4 nm. The cumulative percentage of drug released was determined as the ratio of the amount of released 5-FU to the amount of 5-FU initially inserted into the dialysis bag. All measurements were performed in triplicates.

2.2.3.1. Drug release kinetics. Kinetic analysis of drug release of 5-FU from different CSNPs was performed using various mathematical models such as zero order and first order models as well as Higuchi's model, Hixson-Crowell cube root law, Baker-Lonsdale equation of time kinetics and Peppas exponential model [36]. The regression coefficient values (R^2) were calculated from the plots of Q vs. t in case of zero order, log (Q_0 - Q) vs. t for first order, Q vs. $t^{1/2}$ for Higuchi model, $Q_0^{1/3}$ - (Q_0 - Q)$^{1/3}$ vs. t for Hixson-Crowell model, 3/2[1-(1-Q/Q_0)$^{2/3}$] vs. t for Baker-Lonsdale model and Q vs. Log t for Peppas model.

Where (Q) is the percentage of released drug at time (t) and (Q_0 - Q) is the remaining percentage of drug after time (t). In Peppas model, the release exponent (n) was also calculated in order to determine the drug release mechanism.

2.2.4. Statistical analysis

Results are presented as mean ± SD. Statistical analysis was performed by means of one-way analysis of variance (ANOVA) followed by LSD's post-hoc test for means comparison. A difference of $P < 0.05$ was considered statistically significant.

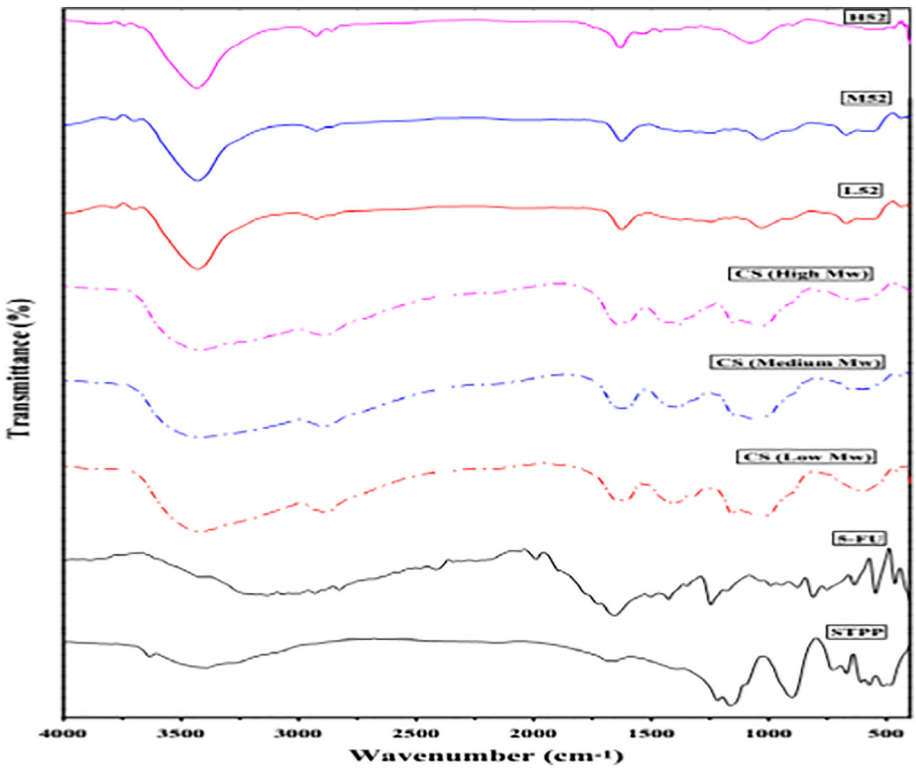

Fig. 1. FTIR spectra of 5-FU, STPP, CS (low, medium and high molecular weight) and CSNPs formulations (L52, M52 and H52).

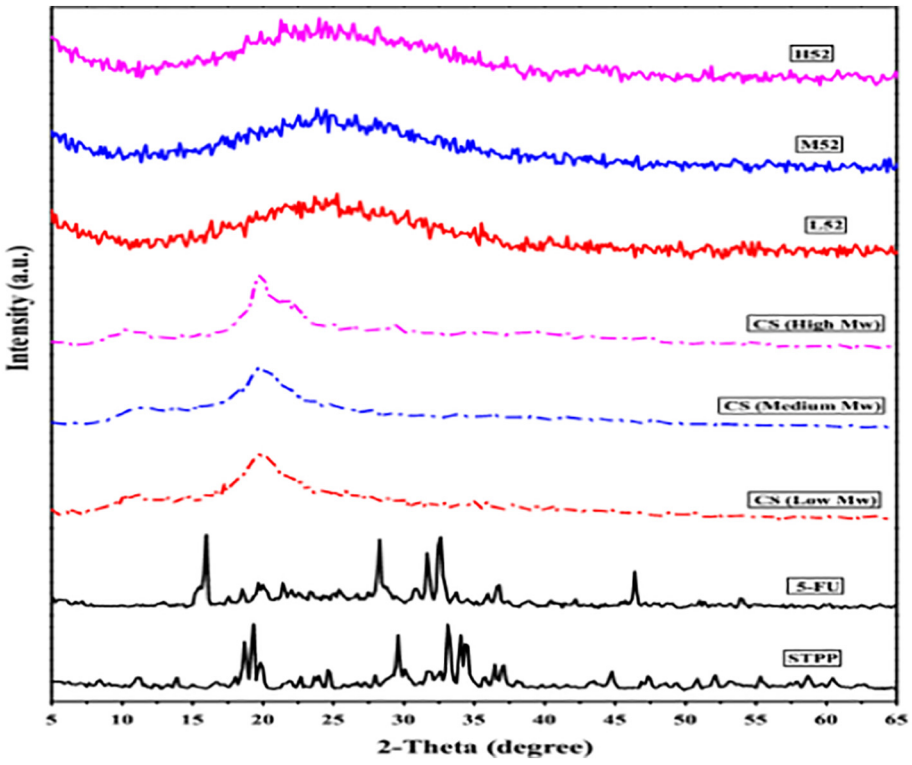

Fig. 2. XRD diffractograms of 5-FU, STPP, CS (low, medium and high molecular weight) and CSNP formulations (L52, M52 and H52).

3. Results and discussion

3.1. Preparation of chitosan nanoparticles

The quick gelling ability of CS in presence of polyanions depends on the formation of both intermolecular and intramolecular crosslinkages mediated by the polyanions [37]. In this study, the preparation of CSNPs was based on the ionic interaction of positively charged CS and negatively charged STPP. The use of STPP as CS crosslinker is a reliable method to produce stable nanoparticles where, during the preparation process, STPP is electrostatically attracted to CS amino groups in order to create ionically crosslinked nanoparticles [38,39]. Previous reports

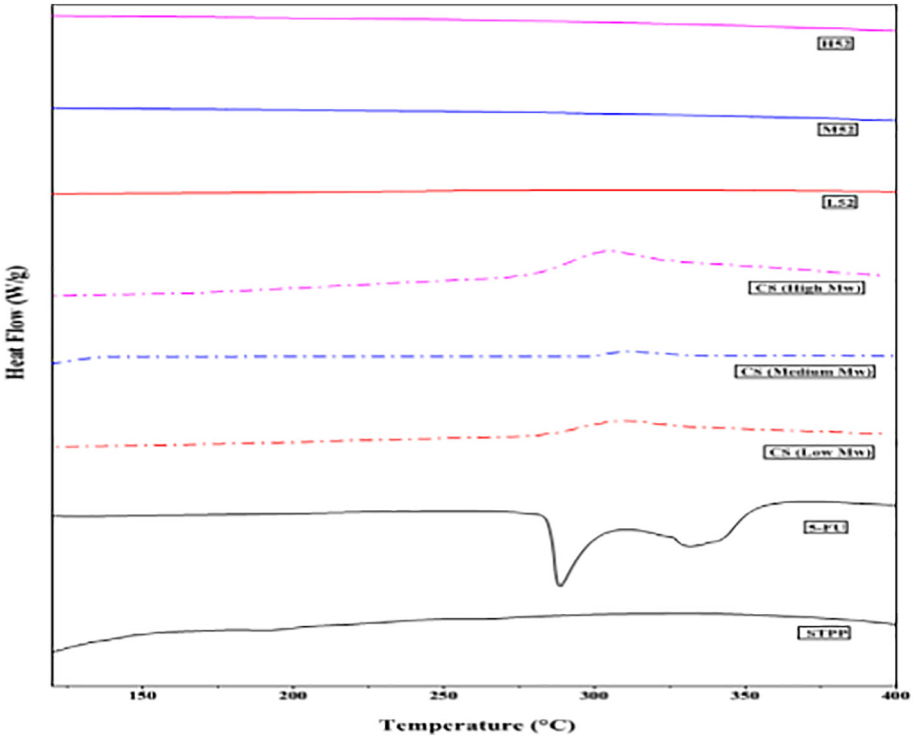

Fig. 3. DSC thermograms of 5-FU, STPP, CS (low, medium and high molecular weight) and CSNPs formulations (L52, M52 and H52).

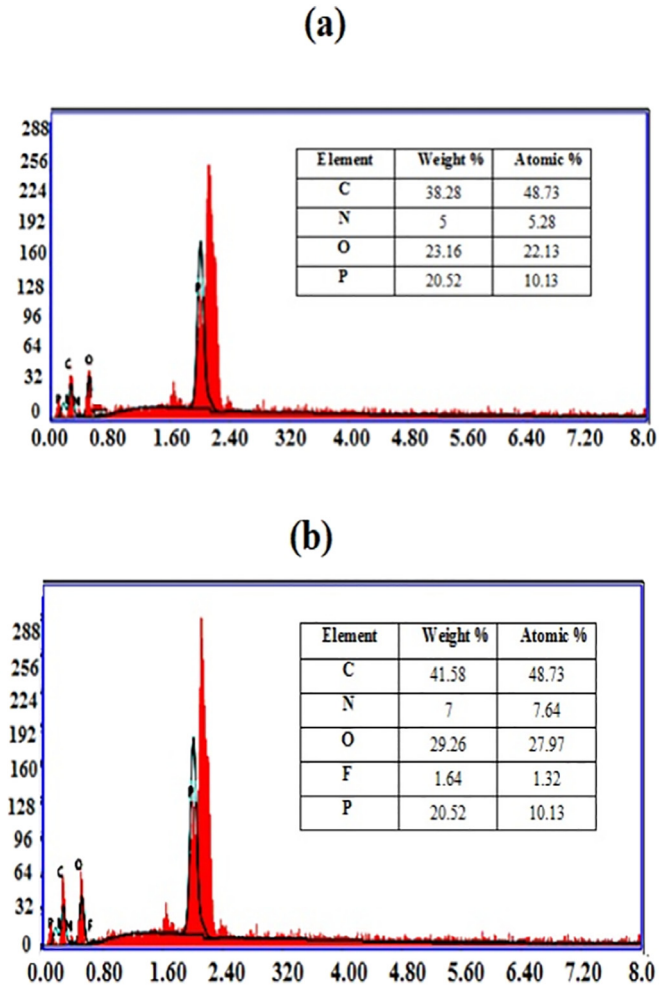

Fig. 4. EDAX analysis of (a) drug free CSNPs formulation L52 and (b) 5-FU loaded CSNPs formulation L52.

showed that the change of the appearance of CS solution upon addition of STPP indicates that there was a change of the physical state of CS from solution to nanoparticles and eventually aggregates [40,41]. Accordingly, the prepared formulations were visually analyzed and identified as either clear solution, colloidal dispersion (which represents the appearance of a suspension of colloidal particels) or aggregation [32], and the results are presented in Table 1. It is clear that the concentration of both CS and STPP as well as CS:STPP mass ratio had a clear effect on the formation of CSNPs. The concentration of CS and STPP should be controlled at a suitable range so as to acheive sucessful formation of CSNPs in the nanosize range [42]. It is obvious that at low STPP concentration (1 mg/ml), no nanoparticles were formed and a clear solution was observed with all CS concentrations tested. Upon increasing STPP concentration to 3 mg/ml, the formation of either nanoparticles or aggrgates depended on the concentration of CS used. In acidic medium, an electrostatic repulsion exists between protonated amino groups of CS molecules. On the other hand, interchain hydrogen bonding between CS molecules is also present. These two forces i.e. intermolecular hydrogen bonding attraction and intermolecular electrostatic repulsion are in equilibrium at low CS concentrations [43]. At higher CS concentrations, as molecules get closer to each other, a limited increase in intermolecular cross-linking takes place. Thus, larger nanoparticles are formed. Further increase in CS concentration will lead to stronger hydrogen bonding interactions, where a plenty of CS molecules become occupied in the cross-linking of a single particle and the electrostatic repulsion between particles is not sufficient to maintain their stability. This leads to formation of larger microparticles which appear as a flocculant precipitate [44].

Another observation is that, in case of low and medium molecular weight CS, higher ability of nanoparticle formation was observed compared to high molecular weight CS (H33 compared to L33 and M33). This can be explained by a decrease in viscosity of the solution as the molecular weight decreases which leads to the simultaneous increase in the ability of CS to form smaller structures [45]. According to the previous observations, nine formulations prepared employing STPP at a single concentration of 2 mg/ml and CS (low, meidum and high molecular weights) at concentrations of 3, 4 and 5 mg/ml were selected for further investigation.

3.2. Characterization of 5-fluorouracil chitosan nanoparticles

3.2.1. Determination of encapsulation efficiency

Table 2 shows the EE% of nine prepared 5-FU loaded CSNPs. Results show that CSNPs displayed EE% values ranging from 3.86% to 21.82%. It is clear that an increase in EE% was observed with the increase of CS concentration from 3 to 5 mg/ml in the three CS molecular weights investigated. The results show that no significant difference in EE% was observed when CS concentration increased from 3 to 4 mg/ml in case of low and high molecular weight CS. On further increase of CS concentration (from 4 to 5 mg/ml), a significant increase in EE% ($P < 0.05$) was observed in the three CS molecular weights investigated. The results indicate that CS concentration as well as CS:STPP ratio, which increased from 3:1 to 5:1, have a prominant effect on the drug's EE% whereas CS molecular weight did not seem to have a clear impact on the EE% of the drug in the investigated formulations. This finding comes in agreement with previous reports. For example, Nagarwal et al. reported an increase in EE% upon increasing CS concentration from 1 to 1.5 to 2 mg/ml

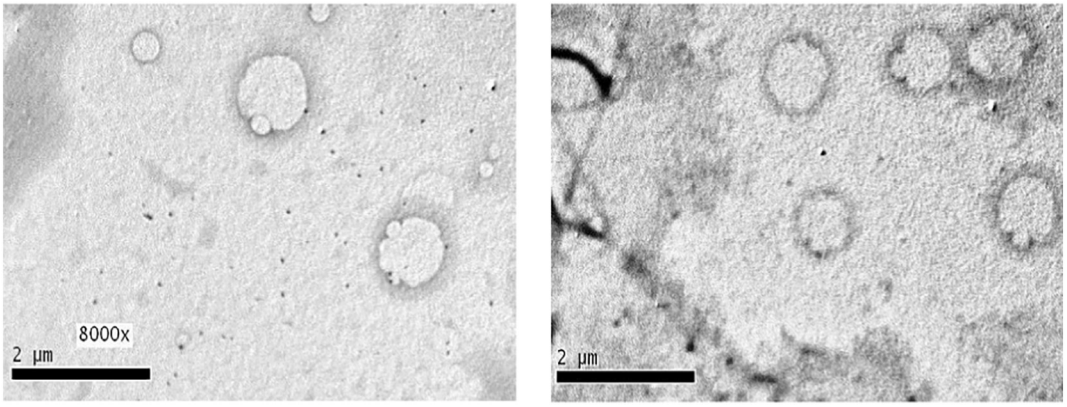

Fig. 5. TEM micrograph of 5-FU loaded CSNPs formulation L52 stained by 1% phosphotungstic acid.

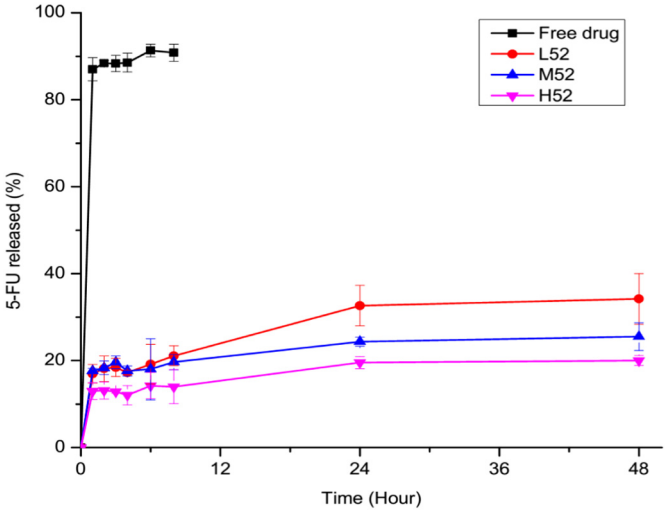

Fig. 6. *In vitro* release profiles of free 5-FU suspension and selected CSNP formulations (L52, M52 and H52) in phosphate buffer, pH 7.4, at 37 °C.

[46]. Mehrotra et al. also reported an increase in EE% with the increase of CS concentration from 1 up to 3 mg/ml. This observed increase in EE% with increasing CS concentration could be attributed to adsorption and electrostatic attraction between the drug and CS molecules [47].

3.2.2. Determination of particle size and polydispersity index

PS values of the prepared 5-FU loaded CSNP formulations were measured and the results are presented in Table 2. The results show that all tested formulations were in the nanosize range with PS ranging from 319.1 to 631.7 nm. The results indicate that PS of CSNPs depended largely on molecular weight of CS. At the same CS concentration, PS of CSNPs increased as higher molecular weight CS was used [37]. CS with lower molecular weight has the tendancy to form smaller nanoparticles as shorter CS chains can easily penetrate into the CS–STPP complexes, resulting in a denser particle. The results also show that a decrease in PS is observed with decreasing the ratio of CS:STPP.

Concerning the effect of CS concentration on PS, a general increase in PS with the increase in CS concentration from 3 to 5 mg/ml is observed. This comes in accordance with previous reports [48,49]. The increase of PS due to the increase in CS concentration could be due to lesser spatial distance between CS molecules at higher concentrations, which leads to the formation of larger particles. On the contrary, smaller PS was obtained with lower CS concentration due to decreased viscosity during ionic gelation [49]. Concerning PDI of the investigated formulations, all CSNPs exhibited PDI values ranging from 0.125 to 0.380 (Table 2). All formulations showed an acceptable PDI (< 0.5) indicating a narrow size distribution [50,51].

Based on the previous results, formulations prepared employing the three molecular weights of CS at a concentration of 5 mg/ml along with STPP at a concentration of 2 mg/ml (i.e. formulations L52, M52 and H52) showed the highest ability to incorporate the drug, exhibiting highest EE%. Also these three formulations were in the nanosize range with suitable PDI values indicating a monodisperse nature, accordingly they were selected for further investigations.

3.2.3. Fourier transform infrared spectroscopy

Fig. 1 displays the FTIR spectra of pure 5-FU, low molecular weight CS, medium molecular weight CS, high molecular weight CS, STPP and the three selected 5-FU loaded CSNPs (L52, M52 and H52). The FTIR spectrum of 5-FU shows intense characteristic peaks at 3178.1, 1725.01, 1655.5, 1426.1, 1245.7, 809.9 and 546.7 cm^{-1} due to the vibration of imide stretch (amide II and amide III) and aromatic ring. Spectral peaks at 3026.7–2929.3 cm^{-1} are due to –C–H stretching bands and at 1348 cm^{-1} due to pyrimidine vibration. Also, the –C–O and –C–N vibrations were observed at 1179.2, 1655.5 and 1245 cm^{-1} [52]. FTIR spectral analysis of STPP showed strong P═O stretching vibrations at 1163.8 cm^{-1}, and P—O stretching at 899.6 cm^{-1} and 727.03 cm^{-1} [49,53]. Similar characteristic peaks were observed in a study presented by Lima et al. [54]. The intense peaks at 1646.9, 1605.4 cm^{-1}; 1647.8, 1601.5 cm^{-1}; and 1647.8, 1604.4 cm^{-1}) are due to N—H bending of amide I and amide II in the chemical structure of low, medium and high molecular weight CS, respectively (Fig. 1). The general characteristic absorption bands of C—N stretching appear at (2881.1, 2880.1 and 2919.7 cm^{-1} in low, medium and high molecular weight CS, respectively [37]. After ionic crosslinking with STPP and incorporation of the drug, the characteristic peaks at ≈ 1646–1647 cm^{-1} for N—H stretching vibration of NH_3^+ group in the CS spectra were shifted to ≈ 1630–1635.4 cm^{-1}. On the other hand, peaks at ≈ 1600–1605 cm^{-1} disappeared (Fig. 1) which could be attributed to the strong ionic interaction between CS and STPP. Concerning the FTIR spectra of L52, M52 and H52, it could be observed that diminishing of the characteristic peaks of 5-FU took place, signifying the interaction between 5-FU and CS molecuoles and indicating successful encapsulation of 5-FU into the prepared nanoparticles.

3.2.4. X-ray diffraction

The XRD patterns of low, medium and high molecular weight CS as well as 5-FU, STPP and 5-FU loaded CSNPs (L52, M52 and H52) are presented in Fig. 2. Low, medium and high molecular weight CS showed strong diffraction peaks at 2θ = 10.8,19.9°; 11.3, 20.3° and 19.9, 22.09°, respectively which indicates the crystalline nature of CS [55]. The XRD pattern of STPP exhibited diffraction peaks at 2θ = 19.4, 33.3 and 34.1°. Intense multiple diffraction peaks were observed at 2θ = 16.1, 19.8, 21.6, 22.1, 28.4, 32.7, 36.7, 36.9 and 46.5° in the diffraction pattern of pure 5-FU indicating that the drug exists in a crystalline state. Although intense peaks were observed in both the polymer and the drug, XRD patterns for selected of 5-FU loaded CSNPs exhibited only broad diffraction peaks (Fig. 2). Disappearance of the distinguished peaks of 5-FU in the spectra of drug loaded CSNPs signify the incorporation of 5-FU within the carrier in an amorphous state [3]. Similar results were also reported for other drugs encapsulated into CS nanoparticles [3,56].

3.2.5. Differential scanning calorimetry

DSC thermograms of selected 5-FU loaded CSNP formulations and their individual components are presented in Fig. 3. DSC technique can provide information concerning physical and chemical properties of the drug incorporated into nanoparticles [57]. DSC detects changes in enthalpy due to changes in the physicochemical properties of a material as a function of temperature. The DSC thermograms of low, medium and high molecular weight CS show exothermic peaks at a temperature

Table 3
The calculated correlation coefficients and kinetics parameters of 5-FU release profile from selected CSNP formulations.

Formulation	Q_{48h} (% ± SD)	Zero order	First order	Higuchi	Hixon Crowell	Baker Lonsdale	Peppas	
		R^2					R^2	n
L52	34.17 ± 5.85	0.8778	0.8832	0.9268	0.8814	0.8940	0.8622	0.2062
M52	25.50 ± 3.19	0.8643	0.8697	0.8921	0.8679	0.8861	0.7902	0.1016
H52	20.01 ± 1.14	0.8981	0.9033	0.9436	0.9016	0.9259	0.8734	0.1413

Q_{48h}: Percent total 5-FU released after 48 h.

of 309.63, 308.64 and 304.18 °C, respectively. These edxothermic peaks are related to the decomposition temperature of the polysaccharide [58]. The DSC thermogram of STPP shows no characteristic thermal transitions which comes in agreement with previous reports [59] and could be attributed to its high melting point (622 °C) [60]. The DSC thermogram of 5-FU exhibits an endothermic peak at 282.80 °C which corresponds to the drug's melting point [61,62]. DSC thermograms of 5-FU loaded CSNP formulations L52, M52 and H52 (Fig. 3) revealed disappearance of the distinguished 5-FU peak. Such finding have been previously reported [3] and could be due to dispersion of the drug within the nanoparticles at molecular level.

3.2.6. Energy dispersive X-ray analysis

EDAX analysis gives information on the element presence of samples. EDAX analysis which indicate that the elemental percentage of the substances present in the area of interst of the prepared drug free CSNPs and 5-FU loaded CSNPs (both for formulation L52) show the labeled peaks in Fig. 4. The precence of carbon (38.82%), nitrogen (5%), oxgen (23.16%), and phosphorus (20.52%) atoms in the areas that was subject to EDAX analysis was observed, and thus the formation of CSNPs was comfirmed in the drug free formulation. The precence of carbon (41.58%); nitrogen (7%); oxgen (29.26%); phosphorus (20.52%), and florine atoms (1.64%), in the areas subjected to EDAX analysis of the drug loaded formulation indicate the formation of 5-FU loaded CSNPs and prescence of 5-FU within the CS matrix was also comfirmed.

3.2.7. Transmission electron microscopy

Fig. 5 shows TEM micrographs of 5-FU loaded CSNP formulation L52. The nanoparticles exhibited a fairly regular dark stained surface, with more or less spherical shape and no signs of aggregation. Their diameters appeared in agreement with the results obtained in the PS determination experiment.

3.3. In vitro drug release

Fig. 6 shows the *in vitro* release profile of 5-FU from three CSNPs; L52, M52 and H52 compared to the free drug suspension. All three CSNP formulations exhibited a sustained release profile where the percentage of 5-FU released after 48 h was 34.17%, 25.51% and 20.01% for L52, M52 and H52, respectively. Conversly, 5-FU suspension showed a relatively fast release, reaching 91.32% after only six hours (Table 3).

Release profiles of the investigated CSNPs showed a biphasic behavior, with an inital fast release was observed for the first hour. This was followed by a sustained, slow release that lasted for up to 48 h. This slow release behaviour of 5-FU was previously reported from CS based carriers [32] and could be attributed to the strong hydrogen bond between drug molecules and CS which retards the diffusion of 5-FU into the release medium. Another important observation is that the percentage of released drug, after 48 h, significantly increased ($P < 0.05$) as the CS molecular weight decreased. A similar behaviour related to CS molecular weight was reported in case of CS based microspheres where an increase in the molecular weight of CS was associated with a more sustained release profile [63].

3.3.1. Drug release kinetics

The release pattern of the investigated CSNPs was found to be most fitted to Higuchi model possessing the highest correlation coefficient (R^2) compared to the other calculated mathematical models (Table 3). This indicates that CSNPs follow diffusion-based release kinetics which comes in agreement with previous reports concerning CSNPs [32]. To further eulcidate the mechanism of drug release, analysis of the release data employing the Peppas equation was performed, and the release exponents "n" was determined. According to Peppas theory, if n is less than or equal to 0.43, then drug release follows Fickian diffusion mechanism. If n lies between 0.43 and 0.85, then the release follows anomalous (non-Fickian) diffusion. Case II transport is expected when $n =$ 0.85, whereas n values > 0.85 indicate super-case II transport. As presented in Table 3, the values of the release exponent "n" were ≤ 0.43 which indicates a Fickian release mechanism. This further confirms that 5-FU release from investigated systems was mainly controlled by a diffusion process.

4. Conclusion

Nanoparticulate drug delivery systems represent a promising strategy with obvious superiority compared to conventional dosage forms because they have the ability to increase drug bioavailability and permeability. In the present study, 5-FU loaded CSNPs were prepared by ionic gelation and a number of parameters that influence the preparation and characteristics of the nanoparticles were investigated such as the molecular weight of CS, concentration of CS and CS:STPP mass ratio. Formation of nanoparticles was successful at STPP concentration of 2 mg/ml with all CS concentrations and molecular weights investigated. EE% of the drug showed a clear increase with increasing the CS concentration. PS of the prepared formulations exhibited a clear increase with increasing CS concentration from 3 to 5 mg/ml. The CS:STPP mass ratio 5:1 exhibited the highest EE% with suitable PS in the nanorange. The results of FTIR, DSC, EDAX and XRD studies confirmed the incorporation of 5-FU within the prepared carriers at molecular level. The release of 5-FU from nanoparticles was biphasic in nature and followed a diffusion based kinetic model. It was also found that using higher molecular weight CS resulted in slower drug release. The obtained results would help in understanding the effect of different factors governing the sucessful formulation of CS based polymeric nanoparticles for efficient delivery of 5-FU.

Author contributions

Moshera Samy**:** Methodology, Investigation, Resources, Writing-Original draft preparation.

Sameh Hosam Abd El-Alim: Methodology, Investigation, Data curation, Writing- Reviewing and Editing, Supervision.

Abd El Gawad Rabia: Visualization, Supervision.

Amal Amin: Conceptualization, Methodology, Visualization, Supervision.

Magdy M. H. Ayoub: Conceptualization, Methodology, Writing-Reviewing and Editing, Visualization, Supervision, Funding acquisition.

Declaration of competing interest

The authors report no declarations of interest.

Acknowledgement

The authors would like to thank Prof. Dr. Mohamed Ali Hassan for his contribution to the present work.

Funding

This work was supported by the National Research Centre, Giza, Egypt on PhD thesis grant no. 1/3/9.

References

[1] A. Salerno, C. Domingo, J. Saurina, PCL foamed scaffolds loaded with 5-fluorouracil anti-cancer drug prepared by an eco-friendly route, Mater. Sci. Eng. C Mater. Biol. Appl. 75 (2017) 1191–1197.

[2] E.A.K. Nivethaa, S. Dhanavel, A. Rebekah, V. Narayanan, A. Stephen, A comparative study of 5-Fluorouracil release from chitosan/silver and chitosan/silver/MWCNT nanocomposites and their cytotoxicity towards MCF-7, Mater. Sci. Eng. C Mater. Biol. Appl. 66 (2016) 244–250.

[3] S. Tummala, M.N. Satish Kumar, A. Prakash, Formulation and characterization of 5-Fluorouracil enteric coated nanoparticles for sustained and localized release in treating colorectal cancer, Saudi Pharm. J. 23 (3) (2015) 308–314.

[4] J.L. Arias, Novel strategies to improve the anticancer action of 5-fluorouracil by using drug delivery systems, Molecules 13 (10) (2008) 2340–2369.
[5] L. Sun, Y. Chen, Y. Zhou, D. Guo, Y. Fan, F. Guo, Y. Zheng, W. Chen, Preparation of 5-fluorouracil-loaded chitosan nanoparticles and study of the sustained release in vitro and in vivo, Asian J. Pharm. Sci. 12 (5) (2017) 418–423.
[6] N. Zhang, Y. Yin, S.J. Xu, W.S. Chen, 5-Fluorouracil: mechanisms of resistance and reversal strategies, Molecules 13 (8) (2008) 1551–1569.
[7] J.L. Arias, M.A. Ruiz, M. Lopez-Viota, A.V. Delgado, Poly(alkylcyanoacrylate) colloidal particles as vehicles for antitumour drug delivery: a comparative study, Colloids Surf. B: Biointerfaces 62 (1) (2008) 64–70.
[8] F.F. Sahle, B. Balzus, C. Gerecke, B. Kleuser, R. Bodmeier, Formulation and in vitro evaluation of polymeric enteric nanoparticles as dermal carriers with pH-dependent targeting potential, Eur. J. Pharm. Sci. 92 (2016) 98–109.
[9] C.E. Mora-Huertas, H. Fessi, A. Elaissari, Polymer-based nanocapsules for drug delivery, Int. J. Pharm. 385 (1) (2010) 113–142.
[10] P. Kumar, K.R. Gajbhiye, K.M. Paknikar, V. Gajbhiye, Chapter 1 - current status and future challenges of various polymers as cancer therapeutics, in: P. Kesharwani, K.M. Paknikar, V. Gajbhiye (Eds.), Polymeric Nanoparticles as a Promising Tool for Anti-Cancer Therapeutics, Academic Press 2019, pp. 1–20.
[11] A. Amin, M. Samy, S.H. Abd El-Alim, A.E.G. Rabia, M.M.H. Ayoub, Assessment of formulation parameters needed for successful vitamin C entrapped polycaprolactone nanoparticles, Int. J. Polym. Mater. Polym. Biomater. 67 (16) (2018) 942–950.
[12] R. Othman, G.T. Vladisavljević, Z.K. Nagy, Preparation of biodegradable polymeric nanoparticles for pharmaceutical applications using glass capillary microfluidics, Chem. Eng. Sci. 137 (2015) 119–130.
[13] S. Wang, H. Chen, Q. Cai, J. Bei, Degradation and 5-fluorouracil release behavior in vitro of polycaprolactone/poly(ethylene oxide)/polylactide tri-component copolymer† 1, Polym. Adv. Technol. 12 (3–4) (2001) 253–258.
[14] R.L. Sastre, M.D. Blanco, C. Teijón, R. Olmo, J.M. Teijón, Preparation and characterization of 5-fluorouracil-loaded poly(ϵ-caprolactone) microspheres for drug administration, Drug Dev. Res. 63 (2) (2004) 41–53.
[15] G. Chen, R. Gong, Study on fluorouracil-chitosan nanoparticle preparation and its antitumor effect, Saudi Pharm. J. 24 (3) (2016) 250–253.
[16] Z. Ma, H.H. Yeoh, L.Y. Lim, Formulation pH modulates the interaction of insulin with chitosan nanoparticles, J. Pharm. Sci. 91 (6) (2002) 1396–1404.
[17] M.A. Mohammed, J.T.M. Syeda, K.M. Wasan, E.K. Wasan, An overview of chitosan nanoparticles and its application in non-parenteral drug delivery, Pharmaceutics 9 (4) (2017).
[18] G. Vozza, M. Danish, H.J. Byrne, J.M. Frias, S.M. Ryan, Application of Box-Behnken experimental design for the formulation and optimisation of selenomethionine-loaded chitosan nanoparticles coated with zein for oral delivery, Int. J. Pharm. 551 (1–2) (2018) 257–269.
[19] H. Zhang, Q. Huang, Z. Huang, T. Liu, Y. Li, Preparation and physicochemical properties of chitosan broadleaf holly leaf nanoparticles, Int. J. Pharm. 479 (1) (2015) 212–218.
[20] T. Banerjee, S. Mitra, A. Kumar Singh, R. Kumar Sharma, A. Maitra, Preparation, characterization and biodistribution of ultrafine chitosan nanoparticles, Int. J. Pharm. 243 (1) (2002) 93–105.
[21] M.H. El-Shabouri, Positively charged nanoparticles for improving the oral bioavailability of cyclosporin-A, Int. J. Pharm. 249 (1) (2002) 101–108.
[22] Y. Xu, Y. Du, Effect of molecular structure of chitosan on protein delivery properties of chitosan nanoparticles, Int. J. Pharm. 250 (1) (2003) 215–226.
[23] J.A. Ko, H.J. Park, S.J. Hwang, J.B. Park, J.S. Lee, Preparation and characterization of chitosan microparticles intended for controlled drug delivery, Int. J. Pharm. 249 (1) (2002) 165–174.
[24] X.Z. Shu, K.J. Zhu, Controlled drug release properties of ionically cross-linked chitosan beads: the influence of anion structure, Int. J. Pharm. 233 (1) (2002) 217–225.
[25] S.A. Agnihotri, N.N. Mallikarjuna, T.M. Aminabhavi, Recent advances on chitosan-based micro- and nanoparticles in drug delivery, J. Control. Release 100 (1) (2004) 5–28.
[26] J. Berger, M. Reist, J.M. Mayer, O. Felt, N.A. Peppas, R. Gurny, Structure and interactions in covalently and ionically crosslinked chitosan hydrogels for biomedical applications, Eur. J. Pharm. Biopharm. 57 (1) (2004) 19–34.
[27] V. Kamat, D. Bodas, K. Paknikar, Chitosan nanoparticles synthesis caught in action using microdroplet reactions, Sci. Rep. 6 (2016) 22260.
[28] P. Zhang, X. Liu, W. Hu, Y. Bai, L. Zhang, Preparation and evaluation of naringenin-loaded sulfobutylether-β-cyclodextrin/chitosan nanoparticles for ocular drug delivery, Carbohydr. Polym. 149 (2016) 224–230.
[29] X.Z. Shu, K.J. Zhu, The influence of multivalent phosphate structure on the properties of ionically cross-linked chitosan films for controlled drug release, Eur. J. Pharm. Biopharm. 54 (2) (2002) 235–243.
[30] P. Calvo, C. Remuñán-López, J.L. Vila-Jato, M.J. Alonso, Novel hydrophilic chitosan-polyethylene oxide nanoparticles as protein carriers, J. Appl. Polym. Sci. 63 (1) (1997) 125–132.
[31] T. Gomathi, P.N. Sudha, J.A.K. Florence, J. Venkatesan, S. Anil, Fabrication of letrozole formulation using chitosan nanoparticles through ionic gelation method, Int. J. Biol. Macromol. 104 (2017) 1820–1832.
[32] R.S.T. Aydin, M. Pulat, 5-fluorouracil encapsulated chitosan nanoparticles for pH-stimulated drug delivery: evaluation of controlled release kinetics, J. Nanomater. 2012 (2012), 42.
[33] V. Zamora-Mora, M. Fernández-Gutiérrez, Á. González-Gómez, B. Sanz, J.S. Román, G.F. Goya, R. Hernández, C. Mijangos, Chitosan nanoparticles for combined drug delivery and magnetic hyperthermia: from preparation to in vitro studies, Carbohydr. Polym. 157 (2017) 361–370.
[34] R.K. Salar, N. Kumar, Synthesis and characterization of vincristine loaded folic acid–chitosan conjugated nanoparticles, Resource-Efficient Technol. 2 (4) (2016) 199–214.
[35] M.M. Badran, M.M. Mady, M.M. Ghannam, F. Shakeel, Preparation and characterization of polymeric nanoparticles surface modified with chitosan for target treatment of colorectal cancer, Int. J. Biol. Macromol. 95 (2017) 643–649.
[36] M. Basha, S.H. Abd El-Alim, A.A. Kassem, S. El Awdan, G. Awad, Benzocaine loaded solid lipid nanoparticles: formulation design, in vitro and in vivo evaluation of local anesthetic effect, Curr. Drug Deliv. 12 (6) (2015) 680–692.
[37] Q. Gan, T. Wang, C. Cochrane, P. McCarron, Modulation of surface charge, particle size and morphological properties of chitosan–TPP nanoparticles intended for gene delivery, Colloids Surf. B: Biointerfaces 44 (2) (2005) 65–73.
[38] H.-C. Yang, M.-H. Hon, The effect of the molecular weight of chitosan nanoparticles and its application on drug delivery, Microchem. J. 92 (1) (2009) 87–91.
[39] F.-L. Mi, S.-S. Shyu, C.-Y. Kuan, S.-T. Lee, K.-T. Lu, S.-F. Jang, Chitosan–polyelectrolyte complexation for the preparation of gel beads and controlled release of anticancer drug. I. Effect of phosphorous polyelectrolyte complex and enzymatic hydrolysis of polymer, J. Appl. Polym. Sci. 74 (7) (1999) 1868–1879.
[40] X.W. Li, D.K.L. Lee, A.S.C. Chan, H.O. Alpar, Sustained expression in mammalian cells with DNA complexed with chitosan nanoparticles, Biochim. Biophys. Acta 1630 (1) (2003) 7–18.
[41] H. Katas, H.O. Alpar, Development and characterisation of chitosan nanoparticles for siRNA delivery, J. Control. Release 115 (2) (2006) 216–225.
[42] J. Zhao, J. Wu, Preparation and characterization of the fluorescent chitosan nanoparticle probe, Chinese J. Anal. Chem. 34 (11) (2006) 1555–1559.
[43] G. Qun, W. Ajun, Effects of molecular weight, degree of acetylation and ionic strength on surface tension of chitosan in dilute solution, Carbohydr. Polym. 64 (1) (2006) 29–36.
[44] W. Fan, W. Yan, Z. Xu, H. Ni, Formation mechanism of monodisperse, low molecular weight chitosan nanoparticles by ionic gelation technique, Colloids Surf. B: Biointerfaces 90 (2012) 21–27.
[45] N. Csaba, M. Köping-Höggård, M.J. Alonso, Ionically crosslinked chitosan/tripolyphosphate nanoparticles for oligonucleotide and plasmid DNA delivery, Int. J. Pharm. 382 (1) (2009) 205–214.
[46] R.C. Nagarwal, P.N. Singh, S. Kant, P. Maiti, J.K. Pandit, Chitosan nanoparticles of 5-fluorouracil for ophthalmic delivery: characterization, in-vitro and in-vivo study, Chem. Pharm. Bull. 59 (2) (2011) 272–278.
[47] A. Mehrotra, R.C. Nagarwal, J.K. Pandit, Lomustine loaded chitosan nanoparticles: characterization and in-vitro cytotoxicity on human lung cancer cell line L132, Chem. Pharm. Bull. 59 (3) (2011) 315–320.
[48] N. Mohammadpour Dounighi, R. Eskandari, M.R. Avadi, H. Zolfagharian, A. Mir Mohammad Sadeghi, M. Rezayat, Preparation and in vitro characterization of chitosan nanoparticles containing Mesobuthus eupeus scorpion venom as an antigen delivery system, J. Venom. Anim. Toxins 18 (1) (2012) 44–52.
[49] M. Agarwal, M.K. Agarwal, N. Shrivastav, S. Pandey, R. Das, P. Gaur, Preparation of chitosan nanoparticles and their in-vitro characterization, Int. J. Life-Sci. Sci. Res. 4 (2) (2018) 1713–1720.
[50] A.A. Kassem, A.M. Mohsen, R.S. Ahmed, T.M. Essam, Self-nanoemulsifying drug delivery system (SNEDDS) with enhanced solubilization of nystatin for treatment of oral candidiasis: design, optimization, in vitro and in vivo evaluation, J. Mol. Liq. 218 (2016) 219–232.
[51] F. Shakeel, N. Haqa, F.K. Alanazi, I.A. Alsarra, Polymeric solid self-nanoemulsifying drug delivery system of glibenclamide using coffee husk as a low cost biosorbent, Powder Technol. 256 (2014) 352–360.
[52] P. Li, Y. Wang, Z. Peng, F. She, L. Kong, Development of chitosan nanoparticles as drug delivery systems for 5-fluorouracil and leucovorin blends, Carbohydr. Polym. 85 (3) (2011) 698–704.
[53] A. Madni, P.M. Kashif, I. Nazir, N. Tahir, M. Rehman, M.I. Khan, M.A. Rahim, A. Jabar, Drug-polymer interaction studies of cytarabine loaded chitosan nanoparticles, J. Chem. Soc. Pak. 39 (6) (2017).
[54] H.A. Lima, F.M.V. Lia, S. Ramdayal, Preparation and characterization of chitosan-insulin-tripolyphosphate membrane for controlled drug release: effect of cross linking agent, J. Biomater. Nanobiotechnol. 5 (4) (2014) 211.
[55] Y. Zhang, Y. Yang, K. Tang, X. Hu, G. Zou, Physicochemical characterization and antioxidant activity of quercetin-loaded chitosan nanoparticles, J. Appl. Polym. Sci. 107 (2) (2008) 891–897.
[56] S. Papadimitriou, D. Bikiaris, K. Avgoustakis, E. Karavas, M. Georgarakis, Chitosan nanoparticles loaded with dorzolamide and pramipexole, Carbohydr. Polym. 73 (1) (2008) 44–54.
[57] Y. Guo, E. Shalaev, S. Smith, Physical stability of pharmaceutical formulations: solid-state characterization of amorphous dispersions, Trends Anal. Chem. 49 (2013) 137–144.
[58] F.J. Caro León, J. Lizardi-Mendoza, W. Argüelles-Monal, E. Carvajal-Millan, Y.L. López Franco, F.M. Goycoolea, Supercritical CO2 dried chitosan nanoparticles: production and characterization, RSC Adv. 7 (49) (2017) 30879–30885.
[59] R.A. Hashad, R.A.H. Ishak, S. Fahmy, S. Mansour, A.S. Geneidi, Chitosan-tripolyphosphate nanoparticles: optimization of formulation parameters for improving process yield at a novel pH using artificial neural networks, Int. J. Biol. Macromol. 86 (2016) 50–58.
[60] M.D. Larrañaga, R.J. Lewis Sr, R.A. Lewis, Hawley's Condensed Chemical Dictionary, 16th ed.
[61] O. Şanlı, A. Kahraman, E. Kondolot Solak, M. Olukman, Preparation of magnetite-chitosan/methylcellulose nanospheres by entrapment and adsorption techniques for targeting the anti-cancer drug 5-fluorouracil, Artif. Cells Nanomed. Biotechnol. 44 (3) (2016) 950–959.

[62] M. Olukman, E.K. Solak, Release of anticancer drug 5-fluorouracil from different ionically crosslinked alginate beads, J. Biomater. Nanobiotechnol. 3 (4) (2012) 469.

[63] Y. Sun, F. Cui, K. Shi, J. Wang, M. Niu, R. Ma, The effect of chitosan molecular weight on the characteristics of spray-dried methotrexate-loaded chitosan microspheres for nasal administration, Drug Dev. Ind. Pharm. 35 (3) (2009) 379–386.